Published in final edited form as:

J Biomed Mater Res B Appl Biomater. 2018 February ; 106(2): 555–568. doi:10.1002/jbm.b.33862.

An engineered macroencapsulation membrane releasing FTY720 to precondition pancreatic islet transplantation

Daniel T. Bowers[1], **Claire E. Olingy**[2], **Preeti Chhabra**[3], **Linda Langman**[3], **Parker H. Merrill**[1], **Ritu S. Linhart**[1], **Michael L. Tanes**[1], **Dan Lin**[1], **Kenneth L. Brayman**[1,3], and **Edward A. Botchwey**[1,2]

[1]Department of Biomedical Engineering, University of Virginia, Charlottesville, Virginia 22903

[2]Wallace H. Coulter Department of Biomedical Engineering, Georgia Institute of Technology and Emory University, Atlanta, Georgia 30332-0363

[3]Department of Surgery, University of Virginia, Charlottesville, Virginia 22903

Abstract

Macroencapsulation is a powerful approach to increase the efficiency of extrahepatic pancreatic islet transplant. FTY720, a small molecule that activates signaling through sphingosine-1-phosphate receptors, is immunomodulatory and pro-angiogenic upon sustained delivery from biomaterials. While FTY720 (fingolimod, Gilenya) has been explored for organ transplantation, in the present work the effect of locally released FTY720 from novel nanofiber-based macroencapsulation membranes is explored for islet transplantation. We screened islet viability during culture with FTY720 and various biodegradable polymers. Islet viability is significantly reduced by the addition of high doses (≥500 ng/mL) of soluble FTY720. Among the polymers screened, islets have the highest viability when cultured with poly(3-hydroxybutyrate-co-3-hydroxyvalerate) (PHBV). Therefore, PHBV was blended with polycaprolactone (PCL) for mechanical stability and electrospun into nanofibers. Islets had no detectable function *ex vivo* following 5 days or 12 h of subcutaneous implantation within our engineered device. Subsequently, we explored a preconditioning scheme in which islets are transplanted 2 weeks after FTY720-loaded nanofibers are implanted. This allows FTY720 to orchestrate a local regenerative milieu while preventing premature transplantation into avascular sites that contain high concentrations of FTY720. These results provide a foundation and motivation for further investigation into the use of FTY720 in preconditioning sites for efficacious islet transplantation.

Keywords

macroencapsulation; islet transplant; immune modulation; FTY720; regenerative medicine

Correspondence to: E.A. Botchwey; edward.botchwey@bme.gatech.edu.

Additional Supporting Information may be found in the online version of this article.

INTRODUCTION

Currently available treatments for insulin-dependent diabetes including insulin injection, finger stick glucose monitoring, insulin infusion by pump and continuous glucose monitoring are not able to achieve the level of control of a properly functioning pancreatic islet. The closed-loop artificial pancreas is on the brink of improving glucose control while also reducing the burden of self-care for diabetes patients; however, a long term curative treatment for diabetes is still under development. Pancreas transplantation, one curative treatment, is a complicated procedure associated with high morbidity and long recovery. Islet transplantation, which does not require open abdominal surgery, has the potential to treat the approximately 6 million Americans who currently use insulin, including those with type 1 and insulin-dependent type 2 diabetes (according to the American Diabetes Association). Pancreatic islet transplantation has recently reached an important multi-center phase 3 trial completion with 87.5% of subjects meeting the primary endpoint.[1] Despite these results, factors including the host immune response (auto- and allo- or xeno-immunity), lack of access to host vasculature for nutrient delivery, and the scarcity of quality donor tissue prevent widespread access to this procedure. Instant blood-mediated inflammatory reaction and the inability to completely remove the transplanted cells, a concern particularly for engineered cell sources, are among the concerns with the clinically-practiced intraportal technique.[2] Alternate sites outside the portal circulation avoid these possible complications and can accommodate larger tissue volumes than are permissible in the liver.[3] Various sites have been explored including intraperitoneal, intramuscular, and subcutaneous locations, as well as immunopriveledged sites such as the eyes, testis, and bone marrow, with the omentum being recently postulated as a superior site compared to the portal circulation due to increased islet revascularization.[4] None of these sites, however, achieve an adequate survival rate given the low numbers of pancreatic islets available for transplantation.[5]

Immunoisolation membranes and materials are designed to protect enclosed cells from the host immune system by providing a physical barrier and are a major component of encapsulation systems. Selectively permeable membranes are designed to permit the passage of nutrients, waste, and small proteins while preventing the passage of immune cells and immunoglobulin. Investigated membranes include hydrogels (predominately alginate[6,7]) and synthetic polymers such as polytetrafluoroethylene[8] and polycaprolactone.[9] Common sites for macroencapsulated and scaffold-supported islets include intraperitoneal/omentum[10,11] and subcutaneous spaces.[12] Encapsulation-based transplantation has not yet performed well enough to warrant replacing the intraportal technique for clinical allogenic islet transplant, but is under clinical investigation with stem cell-derived transplants.[13–16] Macroencapsulation is of particular interest when transplanting engineered or alternate source cells since a macro-device can be completely removed should an adverse immune reaction occur or a teratoma form.[17] With these findings in mind, this study seeks to improve transplanted islet survival using a drug-loaded membrane.

Incorporation of synthetic or endogenously-occurring molecules can direct desired biological responses to foreign materials, which has been demonstrated in the context of tissue engineered devices for islet transplantation.[18] Tissue engineered devices have been

loaded with factors designed to activate signaling networks[19] involved in regenerative processes including vascular endothelial growth factor (VEGF),[20] platelet-derived growth factor (PDGF),[21,22] transforming growth factor-beta 1 (TGF-β1),[23] and sphingosine-1-phosphate.[24] Sphingosine-1-phosphate (S1P) is a pleiotropic autocrine and paracrine signaling lipid that regulates the behavior of endothelial cells,[25,26] smooth muscle cells,[27,28] stem cells,[29] and immune cells[30–32] through its activity at five G-protein-coupled cell surface receptors (S1P1-S1P5). The small molecule FTY720 displays a longer half-life *in vivo* than S1P and mimics the activity of S1P by activating signaling through S1P1, S1P3, S1P4 and S1P5. FTY720 has been investigated as an alternative to the classic immunosuppressive drugs, owing in part to its ability to sequester lymphocytes in secondary lymphoid tissues when administered systemically.

Local delivery of FTY720 from biodegradable polymer scaffold films stimulates increases in local functional vascular length density, arteriolar diameter, and vascular branching by recruiting non-classical anti-inflammatory monocytes.[33,34] Furthermore, we have previously shown that locally released FTY720 from PLGA-PCL nanofibers significantly increases revascularization during mandibular bone defect healing compared to unloaded controls.[35] The present manuscript investigates local release of FTY720 for the specific application of islet transplantation. Electrospun nanofibers can be used to limit cellular migration into the bulk material to approximately 2–3 cell lengths or scaffold layers, which is normally considered a disadvantage for scaffold performance.[36–41] As an encapsulation membrane however, electrospun nanofibers may provide a barrier to inflammatory cell infiltration. Leveraging the immunomodulatory and pro-angiogenic properties of FTY720, we develop a new encapsulation membrane for islet transplantation in locations outside the portal circulation.

MATERIALS AND METHODS

Preparation and characterization of nanofibers

Nanofibers were electrospun from polymer solutions of polyhydroxybutyrate (PHB), poly(3-hydroxybutyrate-co-3-hydroxyvalerate) (PHBV, PHB 95/PHV 5; Carbomer, part # 80181–31-3, lot# 11-SD658), poly(lactic-co-glycolic acid) (PLGA, 50:50 LA:GA, Lakeshore Biomaterials, Birmingham, AL, USA), and polycaprolactone (PCL; Sigma, USA) with or without FTY720 (Cayman Chemical, Ann Arbor, Michigan). Electrospinning parameters are presented in Table I. For each polymer solution, a given driving voltage was applied to an 18G blunt-tipped needle while a syringe pump (World Precision Instruments, Sarasota, FL, USA) drove the polymer solution from a syringe at the given flow rate. All samples were collected on aluminum foil at the indicated distance from the tip and dried at room temperature before use. Fibers prepared for transplantation were collected with intermittent application of salt to increase the porosity of the fibers by dissolving the salt particles before use.

Characterization of nanofibers

Nanofiber diameter and morphology were measured from images gathered on a JEOL 6400 scanning electron microscope (SEM) with Orion image processing. Samples were coated

with gold and then imaged at a working distance of 39–43 mm and an accelerating voltage of 15 kV. Diameter was assessed using ImageJ (NIH, USA, imagej.nih.gov).

To characterize nanofiber strength, three samples from each nanofiber type were subjected to tensile strength testing using an Instron materials testing instrument (Instron Model 5543; Instron Worldwide Headquarters, Norwood, MA). The BlueHill2 Program Software (version 2.14) was used to obtain force-displacement graphs for each sample. Dimensions of each sample (length, width, thickness) were measured prior to testing. The force-displacement curve data was used to calculate engineering stress and strain. Stress (MPa) was calculated by dividing load (N) by cross-sectional area (width × thickness; mm^2). Strain was calculated by evaluating the percent extension, or extension (mm) divided by length (mm). Ultimate Tensile Strength (UTS) was determined as the highest point on the stress-strain curve. Young's Modulus (E) was determined by regression fitting the linear region on the stress-strain curve and evaluating the slope. Values for E and UTS were averaged across samples for each condition.

Hydrophobicity of each nanofiber condition was quantified through contact angle measurements. A drop of the indicated liquid was placed on top of the nanofibers for each condition. A goniometer (Rame-Hart Standard Contact Angle Goniometer, Model 200; Rame-Hart Instrument Co., Succasunna, NJ) and DROPimage Standard software were used to measure the contact angle between the fiber and the liquid.

Islet isolation

Murine pancreatic islets were isolated from C57BL/6J mice (Jackson Laboratories, Bar Harbor, ME), or a donor expressing GFP in all cells including the pancreatic islets, as previously described.[42] Briefly, after confirmation of euthanasia, the common bile duct was occluded using suture and was cannulated with a 30G needle for injection of 2–3 mL of 1.4 mg/mL collagenase P (Roche) dissolved in Hank's Balanced Salt Solution (HBSS, Thermo Scientific) supplemented with 10 mg/L heat treated bovine serum albumin and 0.35 g/L sodium bicarbonate (supplemented HBSS). Incubation in a 37°C water bath was followed by vigorous shaking by hand to disrupt tissue structure. Two washes in supplemented HBSS were followed by filtering through a steel mesh and density separation with Histopaque 1077 (Sigma). Two more washes and a wash in fully supplemented culture media (RPMI1640 + 10% FBS, 2% Penicillin/Streptomycin + 2.5% HEPES) completed the isolation. The islets were cultured in fully supplemented media at 37°C and 5% CO_2 until use (~24 h).

Human islets were isolated using a modified Ricordi method, according to the University of Virginia Center for Cellular Therapy and Biologic Therapeutics Standard Operating Procedures. Briefly, the pancreas was digested with a collagenase based enzyme solution (GMP grade, Roche), purified on a density gradient and washed before being cultured in Miami media 1A (Mediatech) supplemented with 0.5% human serum albumin. Islets were cultured at 37°C and 5% CO_2 until use (~48 h).

FTY720 dose response

FTY720 was solvated in 100% ethanol to a concentration of 2 mg/mL. A stock solution was made by mixing with diH_2O in a 1:1 volume ratio. The islets were incubated for 18 h at

37°C. The FTY720-laden media was removed with the first wash as described for GSIS below. Following the GSIS procedure the islets were stained for viability with propidium iodide (PI). A 5X image for each well was used to quantify the fluorescence intensity in ImageJ. The mean fluorescence intensity was calculated for each well and then averaged for all groups.

Glucose stimulated insulin secretion (GSIS) and viability staining

Islets that had been exposed to FTY720 or polymer used to fabricate the nanofiber membranes were washed once with low glucose (2.8 m*M*) Krebs Ringer's Buffer (KRB) to remove the culture media and placed in the incubator for an hour. Two more washes in low glucose KRB were then performed to start the 2-h incubation at 37°C in low glucose. Samples were then collected, immediately placed on ice and then stored in the freezer. The islets were washed in low glucose twice followed by addition of high glucose (28 m*M*) for the next 2-h incubation. Again samples were taken and frozen until analysis. Low glucose KRB was added to prepare for viability staining. For the *ex vivo* pocket challenge experiment, single pockets loaded with islets were implanted in mice for 12 h or 5 days. The implants were removed intact from the animal and challenged *in vitro*.

PI alone was added to the islets for the FTY720 dose response experiment or in conjunction with fluorescein diacetate (FDA) for the polymer incubation experiments. Imaging was conducted with UV excitation and a red and green fluorescent filter on an inverted Zeiss microscope with a Zeiss Axiocam color camera. Image analysis for the polymer assays was by visual inspection to estimate percentage viability of individual islets, while the FTY720 dose response was based on the PI fluorescence intensity.

ECM dimensional stability

Acellular porcine dermis (ENDURAGen®) and acellular human cadaveric dermis (AlloDerm®) were cut into 1 cm × 1 cm squares and kept at the supplied thickness of approximately 1 mm. Following implantation in distinct subcutaneous pockets in a Sprague-Dawley rat for 4, 8, and 12 weeks, implants were harvested and fixed in 4% paraformaldehyde for 48 h and subsequently kept in 70% ethanol. Extraneous tissue was removed under a stereomicroscope. The longest two axes were measured in images and the aspect ratio was calculated. Therefore, a value near to 1 indicated a square shape, while values further from one indicated a rectangular shape.

Macroencapsulation device construction

Device fabrication was completed in a laminar flow hood to maintain aseptic implants. A rectangular mat of fibers (2 cm wide) was soaked in 70% ethanol and peeled from the aluminum foil collector. The piece was folded over to form a 1- cm wide two-layer mat. Once dry, these folded fibers were heat-sealed at 1-cm intervals using the edge of a metallic plate heated in an oven (125°C) or on a hot plate. After cutting at the midpoint of the heat-seals, pockets were formed (~1 cm^2); each pocket having one folded side, two heat-sealed sides, and one open side (opposite the folded side) (Supporting Information Figure S1). Pockets were incubated in a FTY720-saturated PBS solution for 18–24 h at 4°C to dissolve away the salt particles used in the salt interspersed nanofibers.

Induction of chemical diabetes and blood glucose monitoring

Diabetes was induced in immune competent male and female C57BL/6 or S1P3 knockout mice (C57BL/6 background) using a single intraperitoneal injection of streptozotocin (STZ) dissolved in citrate buffer (pH ~4–5). Function of the implanted islets was monitored by daily glucose readings following transplant. Blood was drawn by tail clip and measured on an Accu-Chek Advantage handheld blood glucose meter (Roche, IN).

Islet implant loading and transplant

After islets were cultured overnight, they were handpicked to increase purity and counted. A "U shaped" piece of Enduragen® decellularized dermis was inserted into the pocket with the "open end" of the insert pointed toward the open end of the pocket. For *in vitro* studies, islets were loaded into the pocket by drawing them into a 200 mL pipet, allowing them to settle to the bottom by gravity and then dispensing them by adjusting the volume specified on the pipet to advance the volume incrementally. The final side was closed via heat sealing, this time using a heated pair of smooth surface hemostats. This same islet loading procedure was followed for subsequent simultaneous islet-implant procedures.

For preconditioning *in vivo* studies, the pocket was constructed with the "U-shaped" insert and the final end was sealed using the heated hemostats. During the first procedure the animal was anesthetized with isoflurane gas (2–3%) and the surgical plane was maintained throughout the procedure with a nose cone (1–2%) equipped with a scavenging apparatus. The hair was removed and the surgical site was washed with iodine and ethanol. An incision through the skin and then through the peritoneal wall was made on the left flank where access to the left kidney can be made. The pocket was inserted into the peritoneal space and a single suture was run though a sealed edge of the pocket to attach it to the inside of the peritoneal wall. Therefore, it contacted the peritoneum on one side and internal organs on the other, usually consisting of a combination of the kidney, spleen, and pancreas. The animal was then sutured using separate sutures for the peritoneal wall and the skin closure. For the second procedure a new incision was made near the previous one to gain access and a clear view of the implant procedure. The pocket was pierced by a needle or 200 μL pipet tip, loaded with the islets by injection and the animal was sutured again. C57BL/6 islets from healthy retired breeders were transplanted into C57BL/6 recipients unless otherwise noted.

All procedures were conducted under an approved Animal Care and Use Committee Protocol at the University of Virginia. Guidelines in the NIH Guide for the Care and Use of Laboratory Animals (NIH Publication, National Academies Press) have been observed.

Histology

Explanted tissue was fixed in buffered formalin for 24 h at room temperature and subsequently kept in 70% ethanol at 4°C before being embedded in paraffin. Tissue specimens were embedded at the University of Virginia Research Histology Core. Sections of the paraffin blocks were cut at 5-micron thickness. Hematoxylin and Eosin (H&E) stain was also completed at the Research Histology Core.

Ultrasound

Animals were placed supine on a heated stage and sedation was maintained with an isoflurane nose cone. Imaging sessions did not last longer than 30 minutes for a given mouse. A Vevo 2100 (VisualSonics, Toronto, Canada) operating at a frequency of approximately 30 MHz was used. Ultrasound gel was placed between the animal's skin and the probe surface. The probe was mounted while the animal/platform could then be translated under the probe to obtain the images shown.

Statistics

A two-tailed Student's *t* test with equal variance or an ANOVA with Tukey's post-test for multiple comparisons was applied as appropriate in Graphpad Prism (Version 6, CA, USA), with a p value <0.05 considered significant.

RESULTS

FTY720-loaded polymer fibers for islet transplantation

Islets near a scaffold releasing FTY720 would experience a high, acute dose of FTY720, as polymer nanofibers promote a burst release profile.[35] Consequently, we investigated islet function in response to soluble FTY720. Increasing concentrations of FTY720 in the culture media were tested from 10 to 1000 ng/mL. Soluble FTY720 concentrations of 500 ng/mL and above significantly reduce murine islet viability [Figure 1(A,B)], while doses of 100 ng/mL and above appear to compromise islet function [stimulation index <2, Figure 1(C)]. The addition of the vehicle control (ethanol) does not have an effect on either metric (Figure S2). These results suggest that high FTY720 concentrations may reduce transplanted islet survival and should be avoided in strategies attempting to leverage angiogenic and immunoregulatory effects of FTY720.

The polymer used in a macroencapsulation membrane will have intimate contact with the isolated islets housed inside. PLGA fibers can be handled better for experiments (greater flexibility and resistance to cracking) when blended with PCL in a 1:1 weight ratio. PLGA and PCL fibers reduce human islet viability [Figure 1(D)]. Islet viability is reduced further by the addition of FTY720 to the PLGA and PCL blend fibers, which agrees with the *in vitro* studies employing soluble FTY720. PHBV, like PLGA, has an adjustable degradation rate based on the ratio of polymerized monomers. In contrast to PLGA, fibers made of PHBV do not reduce human islet viability compared to the media only controls [Figure 1(D)]. PCL-only fibers also do not reduce the viability of co-cultured human islets, supporting the hypothesis that PLGA is responsible for the observed reduction in viability, even when blended with PCL. We chose to blend two of the most islet compatible polymers, PHBV and PCL (PHBV-PCL), for further studies. The combination of PHBV and PCL has been shown to support cellular viability, proliferation and behavior to a similar degree as PHBV or PCL alone.[43,44] PHBV demonstrated more batch-to-batch variability in terms of fiber morphology. A fiber mat composed of PHBV-PCL was more easily heat sealed due to the higher thermal stability of PCL.[45] PHBV-PCL was also more easily handled in the processes of loading islets and surgical implantation without tearing due to increased ductility of a blend containing PCL.[46] Since PHBV is a dual component polymer, the ratio

of PHBV monomers can be varied in further development of this membrane to tune the degradation characteristics.[47]

Morphological comparison of PHBV-PCL fibers with and without FTY720 by scanning electron microscopy reveals little effect from the addition of FTY720 [Figure 2(A)]. The diameter was not significantly affected by the addition of FTY720 (516 ± 236 and 451 ± 211 nm for PHBV/PCL and PHBV/PCL + FTY720, respectively). An increasing trend in both the Young's Modulus and Ultimate tensile strength when the fibers contained FTY720 was observed [Figure 2(B,C)]. Young's moduli of this order of magnitude are similar to organs and soft tissues,[48] suggesting mechanical compatibility once implanted. The contact angle of both water and glycerin were decreased by the addition of FTY720 to the fibers (Table II), suggesting that some of the loaded FTY720 locates to the surface of the fibers, where the hydrophobic tail becomes buried in the polymer chains and the hydrophilic head changes the surface chemistry. Thus, PHBV-PCL fibers demonstrated the mechanical and physical properties that would suggest they are compatible with islet delivery.

FTY720 is a known agonist of S1P1 and S1P3. Considering the role of S1P3 in recruitment of anti-inflammatory macrophages,[34] the expression of S1P1-S1P4 on mouse pancreatic islets,[49] the involvement of sphingosine kinase in responding to high-glucose stress,[50] and the protective effect of S1P2 in the development of STZ diabetes,[51] we investigated whether S1P3 is involved in the development of STZ diabetes. We monitored progression to diabetes in the chemical model comparing wild-type C57BL/6 and S1P3−/− mice. Loss of S1P3 expedites the progression to diabetes in both male and female mice following injection of STZ (Figure 3), indicating that signaling through S1P3 helps protect against diabetes. Conversely, this suggests that increases in S1P3 signaling through FTY720-mediated pharmacological activation may further protect islet function.

Design of a nanofiber pocket for islet transplantation

Islets have a three-dimensional spheroidal shape that an engineered encapsulating device should support. We developed a design where nanofibers surround a protected space formed by another material that enables maintenance of islet three-dimensional structure [Figure 4(A)]. Heat sealing was used as an industrially applicable method to form the nanofiber pocket closures to produce a continuous membrane [Figure 4(B)]. A material that could prevent the fibers and surrounding tissue from collapsing on the enclosed islets became necessary after islets were pressed into the fibers during initial attempts, resulting in a loss of the intra-islet cell-cell contacts. The aspect ratio of two clinically available decellularized ECM products were compared following subcutaneous implantation in rats. The porcine decellularized dermis (Enduragen®) is dimensionally stable over the course of 12 weeks, while human decellularized dermis (Alloderm®) contracts anisotropically by 12 weeks [Figure 4(C,D)]. Therefore, the porcine decellularized dermis was selected for use as the interior support. It was cut into a "U shape" where the long "arms" of this insert are on either side of the islets [Figure 4(A)]. This creates a space in the center of the device, accessible from the open side of the "U", where islets can be housed without mechanical stress. Short-term islet function was assayed to validate the device design.

Islets from a green fluorescent protein (GFP)-expressing murine donor were encapsulated between two layers of nanofibers (no decellularized support) and imaged up to 48 h. The endogenous fluorescence from the GFP decreased over time, suggesting that the islets disaggregated and became less viable when only nanofibers are used without the porcine decellularized dermis structural support [Figure 4(E)]. Islets transplanted in the same procedure as the pocket, termed simultaneous, removed after 12 h or 5 days and challenged with glucose *in vitro*, displayed little function [Figure 4(F)]. Islets placed within the pocket and cultured *in vitro* also displayed a loss of stimulated insulin secretion, indicating that the pocket itself may be impairing islet viability *in vitro* [Figure 4(G)]. Furthermore, islets cultured outside the pocket, but in the same well as the pocket nanofibers (co-culture) [Figure 4(G)], display a reduced responsiveness to glucose, suggesting that buildup of degradation products in a static culture media can impact islet viability. Therefore, poor *in vitro* results may be partly related to inefficient waste and polymer degradation product removal in static culture and future experiments may require perfusion culture or a gel to prevent immediate contact with the bare fibers. Together these data indicate that the environment inside the device is not hospitable to islets *in vitro* or with a simultaneous transplantation scheme.

Preconditioned nanofiber pocket for islet transplant

In order to take advantage of the pro-angiogenic effects of locally-released FTY720, and to avoid the detrimental effects of high dose soluble FTY720, a preconditioning method was employed. In this model, the pocket was implanted without any islets followed by a preconditioning period lasting weeks to months. A second procedure where islets are transplanted into the preconditioned nanofiber pocket can then be performed to treat the hyperglycemia. When implanted subcutaneously, the void within the pocket is maintained for at least 3 months (longest time point observed in this study), as visualized under ultrasound [Figure 5(A)] and histologic staining [Figure 5(B)]. In agreement with our previous findings using PLGA fibers in moderately diabetic animals,[52] examination of the vasculature in the peritoneal wall of a subcutaneously-placed fiber mat shows an increase in adjacent tissue vasculature when the nanofibers are loaded with FTY720 compared to the unloaded control [Figure 5(C)]. Additionally, a pocket placed in the peritoneal space has a layer of vascularized tissue attached at the experiment conclusion [Figure 5(D)]. Although the fibers are porous, we have found no indication that blood vessels will penetrate the membrane by examining histological sections stained for H&E [Figure 5(E)].

A preconditioning scheme is more practical to implement if islet transplantation can be performed in an outpatient procedure. A 28G needle imaged at the void space provides proof of concept for a minimally invasive ultrasound guided transplant procedure [Figure 6(A)]. Preliminary syngeneic islet transplants were conducted with and without the preconditioning scheme [Figure 6(B)]. Islets implanted into the peritoneal space of STZ diabetic mice show that only the preconditioning scheme results in a return to normoglycemia, similar to islets implanted under the kidney capsule or intraperitoneally without macroencapsulation [Figure 6(C,D)]. Removal of the pockets is followed by a return to hyperglycemia at the end of the study period, suggesting that islets within the pocket are responsible for the corrected blood

glucose. Therefore, a preconditioned space created by the FTY720 releasing nanofiber pocket may be effective as an extrahepatic islet transplant site.

DISCUSSION

Overcoming the acute inflammatory phase around implanted devices remains a challenge for implant success in tissue engineering. Anti-inflammatory drugs have been investigated for their ability to suppress adverse inflammatory reactions to biomaterials and transplanted tissues.[53–56] FTY720 is an FDA-approved drug used for clinical treatment of multiple sclerosis under the trade name Gilenya. Additionally, FTY720 has been investigated as an alternative to the immunosuppressive drugs used in whole organ transplantation, but did not receive FDA clearance for this application. The studies described in this manuscript explore the use of FTY720 to improve macroencapsulation membranes in the context of islet transplant. Using FTY720 to aid islet transplantation has been proposed elsewhere.[57] These studies extend this idea to a new macroencapsulation membrane with locally released FTY720 and suggest that careful investigation is required to properly harness S1P signaling for biomaterial-aided islet transplantation.

The pro-angiogenic and immunomodulatory effects of local FTY720 delivery make it an attractive strategy to create an oxygenated and tolerated environment for islet transplantation. Others have found FTY720 to have little detrimental effect on islets. No significant effect on stimulation index was found when islets were treated with 10 and 1000 ng/mL FTY720 at 22°C and 5%CO_2 for a 48 h treatment.[58] This group also found a significant reduction in apoptosis with a 10 ng/mL dose *in vitro* and no significant effect on transplanted human islet function when mice were administered 1 mg/kg/day FTY720 by oral gavage.[58] Similarly, murine stimulation indices were slightly increased by incubation with both 10 n*M* (3.439 ng/mL) and 1 μ*M* (343.9 ng/mL) FTY720 concentrations when incubated at 37°C in glass tubes (SI: 3.03, 4.11 and 4 for 0, 10 and 1000 n*M* FTY720 respectively, calculated from Ref. 59). Differences in islet type, media, drug treatment, and protocol may contribute to the differences observed in our work and previous studies, and indicate that further investigation may be needed.[58,59] Based on our finding of decreased murine islet health with increasing FTY720 concentration (Figure 1), we chose a preconditioning approach that would allow the local concentration of FTY720 to be reduced before islets are infused.

FTY720 is released as the polymer swells and degrades, which likely creates a high concentration of FTY720 immediately surrounding the scaffold. When two sheets of nanofibers were placed subcutaneously on opposite sides of a mouse, there was a reduced inflammatory macrophage content around the FTY720-releasing fibers as compared to the unloaded ones in each mouse.[35] Inflammatory cytokines were also reduced by local release of FTY720 from polymers in subcutaneous tissue.[34,35,60] These data suggest that both the proangiogenic and immunomodulatory effects of S1P signaling are truly localized to the surrounding tissue. Preconditioning with FTY720 treatment has proven effective in models of graft versus host disease where dendritic cells are key players in alloantigen presentation,[61] similar to allogenic islet transplant[62] and further motivating our choice to deliver FTY720 prior to the introduction of cells. Although only preliminary *in vivo*

experiments have been conducted thus far with the nanofiber pocket, only the preconditioning method has restored normoglycemia, confirmed via removal of the implant (Figure 6).

Prevascularized implants have been investigated to reduce the hypoxic damage caused by a lack of blood vessels at the early stages of a transplant. While this is part of the strategy we have employed, delivery of FTY720 has the unique advantage of potential pleiotropic effects during islet transplantation. Based on our previous studies,[33–35,52] FTY720 local delivery promotes vascularization and anti-inflammatory myeloid cell recruitment, which may play key roles in transplant success. Witkowski et al. transplanted syngeneic islets into an intramuscular site that had been preconditioned by local release of VEGF and PDGF, resulting in a higher cure rate than untreated or non-growth factor controls.[63] de Vos et al. investigated a prevascularized expanded polytetrafluoroethylene physical support that was coated with acidic fibroblast growth factor and implanted in the peritoneal cavity 4 weeks prior to islets being introduced, resulting in a higher cure rate compared to no scaffold.[64] Juang et al. found only a modest effect of pre-vascularization when there were no proangiogenic molecules delivered from the implant.[12] In contrast, studies employing FTY720 local delivery enable investigation of additional benefits beyond vascularization, such as modulation of inflammation after allogenic transplantation.

When cells are within a macroencapsulation device, scaffold contraction could disrupt the three-dimensional arrangement of cells. In the case of pancreatic islets, the spherical shape of the aggregate of beta, alpha, delta, PP and epsilon cells has been characterized[65–67] and is important for optimal glucose control.[68–70] Cross-linked porcine decellularized dermis (Enduragen®) is dimensionally stable, allowing it to prevent pocket collapse during site preconditioning as well as post-transplantation. The protected space within the device was confirmed using non-invasive ultrasound out to 12 weeks following subcutaneous implantation (Figure 5). In future work, encapsulating the islets in a hydrogel or in microcapsules inside the device would be an alternative way to support the spherical shape of islets within the device. Nanofibers have been used to encourage aggregation of individual cells into pseudo-islets,[71,72] underscoring possible extension of nanofibers as a macroencapsulation material for stem cell-derived islets. Local release of FTY720 may also benefit other encapsulation designs,[18] including scaffoldless approaches[17] and porous scaffolding techniques.[73,74]

Revascularization of transplanted pancreatic islets is critical to the efficient and long-term restoration of normoglycemia. While pancreatic islets are known to produce angiogenic factors such as VEGF, hypoxia still occurs immediately post-transplantation. Hypoxia induces islet necrosis, caused by insufficient diffusion-limited nutrient delivery, which then contributes to a significant loss of functional tissue. Since the largest islets are affected first, one method to address this challenge has been to engineer islets of a sufficiently small size.[75–78] The cost of extended culture times and the requirement of disaggregation may be drawbacks to this approach when using primary cells. Other approaches at various stages of development include genetic engineering of the islets to produce angiogenic factors, co-transplantation of endothelial cells or other proangiogenic cells, site preconditioning (as investigated in the present work),[63,79] and direct oxygen supply.[80]

Preconditioning has proven useful in multiple islet implant systems,[81–84] highlighting the utility of this technique. In the present study, two weeks is sufficient for a significant amount of FTY720 to be released, exert its therapeutic effects, and be cleared from the transplant site in preparation for islet transplantation.[35] Investigations of the Theracyte device showed that a preimplantation period of 3 months significantly improved the cure rate and reduced the numbers of islets required to effect a cure.[85] Addition of pleiotropic molecules such as FTY720 to condition transplant sites within similar devices could be an effective way to further improve islet survival and functionality. Although there may be an additional cost in performing a two-step procedure, other clinically-relevant macroencapsulation devices are rechargeable (MAILPAN, Defymed), suggesting feasibility of multiple clinic visits. Furthermore, this nanofiber device is compatible with simple and safe monitoring methods such as ultrasound and optical imaging techniques, which can be used to monitor the device during the preconditioning period and following the pancreatic islet delivery procedure for parameters including oxygenation.[86]

In summary, we have developed a novel drug-releasing nanofiber-based semi-permeable membrane for the application of pancreatic islet transplantation. The experiments suggest that nanofibers composed of PHBV and PCL are compatible with islets, while PLGA may release degradation products that impair islet function. FTY720 delivery may provide several benefits if delivered to transplantation sites; however, high doses of FTY720 appear to be toxic to islets. Consequently, a preconditioning implant scheme prevents exposure of islets to harmful concentrations of FTY720, while simultaneously leveraging its therapeutic effects. During this preconditioning period, local release of FTY720 promotes a regenerative environment, supporting use of FTY720 in tissue engineering-based approaches to improve cell transplantation.

Supplementary Material

Refer to Web version on PubMed Central for supplementary material.

Acknowledgments

The authors thank Nate Sarbin for expertise in human islet isolation and culture as well as stimulating conversation regarding this work. They also thank Yong Lin and Nicole Keane for data collection assistance. Ultrasound equipment time was kindly given by Dr. John Hossack at the University of Virginia.

Contract grant sponsor: National Science Foundation; contract grant number: 0933643

References

1. Hering BJ, Clarke WR, Bridges ND, Eggerman TL, Alejandro R, Bellin MD, Chaloner K, Czarniecki CW, Goldstein JS, Hunsicker LG, Kaufman DB, Korsgren O, Larsen CP, Luo X, Markmann JF, Naji A, Oberholzer J, Posselt AM, Rickels MR, Ricordi C, Robien MA, Senior PA, Shapiro AM, Stock PG, Turgeon NA, Clinical Islet Transplantation Consortium. Phase 3 trial of transplantation of human islets in type 1 diabetes complicated by severe hypoglycemia. Diabetes Care. 2016; 39:1230–1240. [PubMed: 27208344]
2. Chhabra P, Sutherland DER, Brayman KL. Overcoming barriers in clinical islet transplantation: Current limitations and future prospects. Curr Probl Surg. 2014; 51:49–86. [PubMed: 24411187]

3. Kawahara T, Kin T, Kashkoush S, Gala-Lopez B, Bigam DL, Kneteman NM, Koh A, Senior PA, Shapiro AM. Portal vein thrombosis is a potentially preventable complication in clinical islet transplantation. Am J Transplant. 2011; 11:2700–2707. [PubMed: 21883914]
4. Espes D, Lau J, Quach M, Ullsten S, Christoffersson G, Carlsson PO. Rapid Restoration of Vascularity and Oxygenation in Mouse and Human Islets Transplanted to Omentum May Contribute to Their Superior Function Compared to Intraportally Transplanted Islets. Am J Transplant. 2016; 16:3246–3254. [PubMed: 27321369]
5. Smink AM, Faas MM, de Vos P. Toward engineering a novel transplantation site for human pancreatic islets. Diabetes. 2013; 62:1357–1364. [PubMed: 23613549]
6. de Vos P, Lazarjani HA, Poncelet D, Faas MM. Polymers in cell encapsulation from an enveloped cell perspective. Adv Drug Deliv Rev. 2014:67–68. 15–34. [PubMed: 24361391]
7. Lim F, Sun AM. Microencapsulated islets as bioartificial endocrine pancreas. Science. 1980; 210:908–910. [PubMed: 6776628]
8. Brauker JH, Carr-Brendel VE, Martinson LA, Crudele J, Johnston WD, Johnson RC. Neovascularization of synthetic membranes directed by membrane microarchitecture. J Biomed Mater Res. 1995; 29:1517–1524. [PubMed: 8600142]
9. Nyitray CE, Chang R, Faleo G, Lance KD, Bernards DA, Tang Q, Desai TA. Polycaprolactone Thin-Film Micro- and Nanoporous Cell-Encapsulation Devices. ACS Nano. 2015; 9:5675–5682. [PubMed: 25950860]
10. Jiang K, Weaver JD, Li Y, Chen X, Liang J, Stabler CL. Local release of dexamethasone from macroporous scaffolds accelerates islet transplant engraftment by promotion of anti-inflammatory M2 macrophages. Biomaterials. 2017; 114:71–81. [PubMed: 27846404]
11. Weaver JD, Song Y, Yang EY, Ricordi C, Pileggi A, Buchwald P, Stabler CL. Controlled Release of Dexamethasone from Organosilicone Constructs for Local Modulation of Inflammation in Islet Transplantation. Tissue Eng Part A. 2015; 21:2250–2261. [PubMed: 26027872]
12. Juang JH, Bonner-Weir S, Ogawa Y, Vacanti JP, Weir GC. Outcome of subcutaneous islet transplantation improved by polymer device. Transplantation. 1996; 61:1557–1561. [PubMed: 8669096]
13. Pagliuca FW, Millman JR, Gürtler M, Segel M, Van Dervort A, Ryu JH, Peterson QP, Greiner D, Melton DA. Generation of Functional Human Pancreatic b Cells In Vitro. Cell. 2014; 159:428–439. [PubMed: 25303535]
14. Vegas AJ, Veiseh O, Gürtler M, Millman JR, Pagliuca FW, Bader AR, Doloff JC, Li J, Chen M, Olejnik K, Tam HH, Jhunjhunwala S, Langan E, Aresta-Dasilva S, Gandham S, McGarrigle JJ, Bochenek MA, Hollister-Lock J, Oberholzer J, Greiner DL, Weir GC, Melton DA, Langer R, Anderson DG. Long-term glycemic control using polymer-encapsulated human stem cell-derived beta cells in immune-competent mice. Nat Med. 2016; 22:306–311. [PubMed: 26808346]
15. Rezania A, Bruin JE, Arora P, Rubin A, Batushansky I, Asadi A, O'Dwyer S, Quiskamp N, Mojibian M, Albrecht T, Yang YH, Johnson JD, Kieffer TJ. Reversal of diabetes with insulin-producing cells derived in vitro from human pluripotent stem cells. Nat Biotechnol. 2014; 32:1121–1133. [PubMed: 25211370]
16. Agulnick AD, Ambruzs DM, Moorman MA, Bhoumik A, Cesario RM, Payne JK, Kelly JR, Haakmeester C, Srijemac R, Wilson AZ, Kerr J, Frazier MA, Kroon EJ, D'Amour KA. Insulin-Producing Endocrine Cells Differentiated In Vitro From Human Embryonic Stem Cells Function in Macroencapsulation Devices In Vivo. Stem Cells Transl Med. 2015; 4:1214–1222. [PubMed: 26304037]
17. Pepper AR, Gala-Lopez B, Pawlick R, Merani S, Kin T, Shapiro AMJ. A prevascularized subcutaneous device-less site for islet and cellular transplantation. Nat Biotechnol. 2015; 33:518–523. [PubMed: 25893782]
18. Bowers DT, Botchwey EA, Brayman KL. Advances in Local Drug Release and Scaffolding Design to Enhance Cell Therapy for Diabetes. Tissue Eng Part B Rev. 2015; 21:491–503. [PubMed: 26192271]
19. Kumbar SG, Nair LS, Bhattacharyya S, Laurencin CT. Polymeric nanofibers as novel carriers for the delivery of therapeutic molecules. J Nanosci Nanotechnol. 2006; 6:2591–2607. [PubMed: 17048469]

20. Trivedi N, Steil GM, Colton CK, Bonner-Weir S, Weir GC. Improved vascularization of planar membrane diffusion devices following continuous infusion of vascular endothelial growth factor. Cell Transplant. 2000; 9:115–124. [PubMed: 10784073]
21. Elliott Donaghue I, Shoichet MS. Controlled release of bioactive PDGF-AA from a hydrogel/nanoparticle composite. Acta Biomater. 2015; 25:35–42. [PubMed: 26257128]
22. Sakiyama-Elbert SE, Das R, Gelberman RH, Harwood F, Amiel D, Thomopoulos S. Controlled-release kinetics and biologic activity of platelet-derived growth factor-BB for use in flexor tendon repair. J Hand Surg Am. 2008; 33:1548–1557. [PubMed: 18984337]
23. Liu JM, Zhang J, Zhang X, Hlavaty KA, Ricci CF, Leonard JN, Shea LD, Gower RM. Transforming growth factor-beta 1 delivery from microporous scaffolds decreases inflammation post-implant and enhances function of transplanted islets. Biomaterials. 2016; 80:11–19. [PubMed: 26701143]
24. Sefcik LS, Petrie Aronin CE, Wieghaus KA, Botchwey EA. Sustained release of sphingosine 1-phosphate for therapeutic arteriogenesis and bone tissue engineering. Biomaterials. 2008; 29:2869–2877. [PubMed: 18405965]
25. Kluk MJ, Hla T. Role of the sphingosine 1-phosphate receptor EDG-1 in vascular smooth muscle cell proliferation and migration. Circ Res. 2001; 89:496–502. [PubMed: 11557736]
26. Lockman K, Hinson JS, Medlin MD, Morris D, Taylor JM, Mack CP. Sphingosine 1-phosphate stimulates smooth muscle cell differentiation and proliferation by activating separate serum response factor co-factors. J Biol Chem. 2004; 279:42422–42430. [PubMed: 15292266]
27. Peng X, Hassoun PM, Sammani S, McVerry BJ, Burne MJ, Rabb H, Pearse D, Tuder RM, Garcia JG. Protective effects of sphingosine 1-phosphate in murine endotoxin-induced inflammatory lung injury. Am J Respir Crit Care Med. 2004; 169:1245–1251. [PubMed: 15020292]
28. Zisch AH, Lutolf MP, Ehrbar M, Raeber GP, Rizzi SC, Davies N, Schmökel H, Bezuidenhout D, Djonov V, Zilla P, Hubbell JA. Cell-demanded release of VEGF from synthetic, biointeractive cell ingrowth matrices for vascularized tissue growth. FASEB J. 2003; 17:2260–2262. [PubMed: 14563693]
29. Golan K, Vagima Y, Ludin A, Itkin T, Cohen-Gur S, Kalinkovich A, Kollet O, Kim C, Schajnovitz A, Ovadya Y, Lapid K, Shivtiel S, Morris AJ, Ratajczak MZ, Lapidot T. S1P promotes murine progenitor cell egress and mobilization via S1P1-mediated ROS signaling and SDF-1 release. Blood. 2012; 119:2478–2488. [PubMed: 22279055]
30. Morris MA, Gibb DR, Picard F, Brinkmann V, Straume M, Ley K. Transient T cell accumulation in lymph nodes and sustained lymphopenia in mice treated with FTY720. Eur J Immunol. 2005; 35:3570–3580. [PubMed: 16285007]
31. Sugita K, Kabashima K, Sakabe J, Yoshiki R, Tanizaki H, Tokura Y. FTY720 regulates bone marrow egress of eosinophils and modulates late-phase skin reaction in mice. Am J Pathol. 2010; 177:1881–1887. [PubMed: 20802177]
32. Wang F, Tan W, Guo D, Zhu X, Qian K, He S. Altered Expression of Signaling Genes in Jurkat Cells upon FTY720 Induced Apoptosis. Int J Mol Sci. 2010; 11:3087–3105. [PubMed: 20957081]
33. Sefcik LS, Aronin CE, Awojoodu AO, Shin SJ, Mac Gabhann F, MacDonald TL, Wamhoff BR, Lynch KR, Peirce SM, Botchwey EA. Selective activation of sphingosine 1-phosphate receptors 1 and 3 promotes local microvascular network growth. Tissue Eng A. 2011; 17:617–629.
34. Awojoodu AO, Ogle ME, Sefcik LS, Bowers DT, Martin K, Brayman KL, Lynch KR, Peirce-Cottler SM, Botchwey E. Sphingosine 1-phosphate receptor 3 regulates recruitment of anti-inflammatory monocytes to microvessels during implant arteriogenesis. Proc Natl Acad Sci U S A. 2013; 110:13785–13790. [PubMed: 23918395]
35. Das A, Segar CE, Hughley BB, Bowers DT, Botchwey EA. The promotion of mandibular defect healing by the targeting of S1P receptors and the recruitment of alternatively activated macrophages. Biomaterials. 2013; 34:9853–9862. [PubMed: 24064148]
36. Nam J, Huang Y, Agarwal S, Lannutti J. Improved cellular infiltration in electrospun fiber via engineered porosity. Tissue Eng. 2007; 13:2249–2257. [PubMed: 17536926]
37. Lee JB, Jeong SI, Bae MS, Yang DH, Heo DN, Kim CH, Alsberg E, Kwon IK. Highly porous electrospun nanofibers enhanced by ultrasonication for improved cellular infiltration. Tissue Eng Part A. 2011; 17:2695–2702. [PubMed: 21682540]

38. Vaquette C, Cooper-White JJ. Increasing electrospun scaffold pore size with tailored collectors for improved cell penetration. Acta Biomater. 2011; 7:2544–2557. [PubMed: 21371575]
39. Gentsch R, Boysen B, Lankenau A, Börner HG. Single-step electro-spinning of bimodal fiber meshes for ease of cellular infiltration. Macromol Rapid Commun. 2010; 31:59–64. [PubMed: 21590837]
40. Baker BM, Gee AO, Metter RB, Nathan AS, Marklein RA, Burdick JA, Mauck RL. The potential to improve cell infiltration in composite fiber-aligned electrospun scaffolds by the selective removal of sacrificial fibers. Biomaterials. 2008; 29:2348–2358. [PubMed: 18313138]
41. Guimarães A, Martins A, Pinho ED, Faria S, Reis RL, Neves NM. Solving cell infiltration limitations of electrospun nanofiber meshes for tissue engineering applications. Nanomedicine (Lond). 2010; 5:539–554. [PubMed: 20528450]
42. Chhabra P, Schlegel K, Okusa MD, Lobo PI, Brayman KL. Naturally occurring immunoglobulin M (nIgM) autoantibodies prevent autoimmune diabetes and mitigate inflammation after transplantation. Ann Surg. 2012; 256:634–641. [PubMed: 22964733]
43. Del Gaudio C, Fioravanzo L, Folin M, Marchi F, Ercolani E, Bianco A. Electrospun tubular scaffolds: on the effectiveness of blending poly(ε-caprolactone) with poly(3-hydroxybutyrate-co-3-hydroxyvalerate). J Biomed Mater Res B. 2012; 100:1883–1898.
44. Thadavirul N, Pavasant P, Supaphol P. Fabrication and Evaluation of Polycaprolactone–Poly(hydroxybutyrate) or Poly(3-Hydroxybutyrate-co-3-Hydroxyvalerate) Dual-Leached Porous Scaffolds for Bone Tissue Engineering Applications. Macromol Mater Eng. 2016; 1600289
45. Mofokeng JP, Luyt AS. Morphology and thermal degradation studies of melt-mixed poly(hydroxybutyrate-co-valerate) (PHBV)/poly(ε-caprolactone) (PCL) biodegradable polymer blend nano-composites with TiO2 as filler. J Mater Sci. 2015; 50:3812–3824.
46. Chiono V, Ciardelli G, Vozzi G, Sotgiu MG, Vinci B, Domenici C, Giusti P. Poly(3-hydroxybutyrate-co-3-hydroxyvalerate)/poly(epsilon-caprolactone) blends for tissue engineering applications in the form of hollow fibers. J Biomed Mater Res A. 2008; 85:938–953. [PubMed: 17896770]
47. Hlavaty KA, Gibly RF, Zhang X, Rives CB, Graham JG, Lowe WL Jr, Luo X, Shea LD. Enhancing human islet transplantation by localized release of trophic factors from PLG scaffolds. Am J Transplant. 2014; 14:1523–1532. [PubMed: 24909237]
48. Akhtar R, Sherratt MJ, Cruickshank JK, Derby B. Characterizing the elastic properties of tissues. Mater Today (Kidlington). 2011; 14:96–105. [PubMed: 22723736]
49. Laychock SG, Tian Y, Sessanna SM. Endothelial differentiation gene receptors in pancreatic islets and INS-1 cells. Diabetes. 2003; 52:1986–1993. [PubMed: 12882914]
50. Cantrell Stanford J, Morris AJ, Sunkara M, Popa GJ, Larson KL, Özcan S. Sphingosine 1-phosphate (S1P) regulates glucose-stimulated insulin secretion in pancreatic beta cells. J Biol Chem. 2012; 287:13457–13464. [PubMed: 22389505]
51. Imasawa T, Koike K, Ishii I, Chun J, Yatomi Y. Blockade of sphingosine 1-phosphate receptor 2 signaling attenuates streptozotocin-induced apoptosis of pancreatic beta-cells. Biochem Biophys Res Commun. 2010; 392:207–211. [PubMed: 20060809]
52. Bowers DT, Chhabra P, Langman L, Botchwey EA, Brayman KL. FTY720-loaded poly(DL-lactide-co-glycolide) electrospun scaffold significantly increases microvessel density over 7 days in streptozotocin-induced diabetic C57b16/J mice: preliminary results. Transplant Proc. 2011; 43:3285–3287. [PubMed: 22099778]
53. Merrell JG, McLaughlin SW, Tie L, Laurencin CT, Chen AF, Nair LS. Curcumin-loaded poly(epsilon-caprolactone) nanofibres: diabetic wound dressing with anti-oxidant and anti-inflammatory properties. Clin Exp Pharmacol Physiol. 2009; 36:1149–1156. [PubMed: 19473187]
54. Laurencin, CT., Khan, Y. Regenerative engineering. Boca Raton: CRC Press/Taylor & Francis; 2013. p. 435
55. Dang TT, Thai AV, Cohen J, Slosberg JE, Siniakowicz K, Doloff JC, Ma M, Hollister-Lock J, Tang KM, Gu Z, Cheng H, Weir GC, Langer R, Anderson DG. Enhanced function of immuno-isolated islets in diabetes therapy by co-encapsulation with an anti-inflammatory drug. Biomaterials. 2013; 34:5792–5801. [PubMed: 23660251]

56. Chhabra P, Wang K, Zeng Q, Jecmenica M, Langman L, Linden J, Ketchum RJ, Brayman KL. Adenosine A(2A) agonist administration improves islet transplant outcome: Evidence for the role of innate immunity in islet graft rejection. Cell Transplant. 2010; 19:597–612. [PubMed: 20350347]
57. Jessup CF, Bonder CS, Pitson SM, Coates PTH. The sphingolipid rheostat: a potential target for improving pancreatic islet survival and function. Endocr Metab Immune Disord Drug Targets. 2011; 11:262–272. [PubMed: 21696364]
58. Truong W, Emamaullee JA, Merani S, Anderson CC, James Shapiro AM. Human islet function is not impaired by the sphingosine-1-phosphate receptor modulator FTY720. Am J Transplant. 2007; 7:2031–2038. [PubMed: 17617868]
59. Fu F, Hu S, Deleo J, Li S, Hopf C, Hoover J, Wang S, Brinkmann V, Lake P, Shi VC. Long-term islet graft survival in streptozotocin- and autoimmune-induced diabetes models by immunosuppressive and potential insulinotropic agent FTY720. Transplantation. 2002; 73:1425–1430. [PubMed: 12023620]
60. Ogle ME, Sefcik LS, Awojoodu AO, Chiappa NF, Lynch K, Peirce-Cottler S, Botchwey EA. Engineering in vivo gradients of sphingosine-1-phosphate receptor ligands for localized microvascular remodeling and inflammatory cell positioning. Acta Biomater. 2014; 10:4704–4714. [PubMed: 25128750]
61. Taylor PA, Ehrhardt MJ, Lees CJ, Tolar J, Weigel BJ, Panoskaltsis-Mortari A, Serody JS, Brinkmann V, Blazar BR. Insights into the mechanism of FTY720 and compatibility with regulatory T cells for the inhibition of graft-versus-host disease (GVHD). Blood. 2007; 110:3480–3488. [PubMed: 17606761]
62. Luo X, Miller SD, Shea LD. Immune Tolerance for Autoimmune Disease and Cell Transplantation. Annu Rev Biomed Eng. 2016; 18:181–205. [PubMed: 26928211]
63. Witkowski P, Sondermeijer H, Hardy MA, Woodland DC, Lee K, Bhagat G, Witkowski K, See F, Rana A, Maffei A, Itescu S, Harris PE. Islet grafting and imaging in a bioengineered intramuscular space. Transplantation. 2009; 88:1065–1074. [PubMed: 19898201]
64. de Vos P, Hillebrands JL, De Haan BJ, Strubbe JH, Van Schilfgaarde R. Efficacy of a prevascularized expanded polytetra-fluoroethylene solid support system as a transplantation site for pancreatic islets. Transplantation. 1997; 63:824–830. [PubMed: 9089221]
65. Ionescu-Tirgoviste C, Gagniuc PA, Gubceac E, Mardare L, Popescu I, Dima S, Militaru M. A 3D map of the islet routes throughout the healthy human pancreas. Sci Rep. 2015; 5:14634. [PubMed: 26417671]
66. Steiner DJ, Kim A, Miller K, Hara M. Pancreatic islet plasticity: interspecies comparison of islet architecture and composition. Islets. 2:135–145.
67. Bosco D, Armanet M, Morel P, Niclauss N, Sgroi A, Muller YD, Giovannoni L, Parnaud G, Berney T. Unique arrangement of alpha- and beta-cells in human islets of Langerhans. Diabetes. 2010; 59:1202–1210. [PubMed: 20185817]
68. Lin C-C, Anseth KS. Cell-cell communication mimicry with poly(-ethylene glycol) hydrogels for enhancing-cell function. Proc Natl Acad Sci. 2011; 108:6380–6385. [PubMed: 21464290]
69. Geron E, Boura-Halfon S, Schejter ED, Shilo B-Z. The Edges of Pancreatic Islet b Cells Constitute Adhesive and Signaling Microdomains. Cell Rep. 2015; 10:317–325.
70. Parnaud G, Lavallard V, Bedat B, Matthey-Doret D, Morel P, Berney T, Bosco D. Cadherin engagement improves insulin secretion of single human β-cells. Diabetes. 2015; 64:887–896. [PubMed: 25277393]
71. Kodama S, Kojima K, Furuta S, Chambers M, Paz AC, Vacanti CA. Engineering functional islets from cultured cells. Tissue Eng A. 2009; 15:3321–3329.
72. Song C, Huang YD, Wei Z, Hou Y, Xie WJ, Huang RP, Song YM, Lv HG, Song CF. Polyglycolic Acid-islet grafts improve blood glucose and insulin concentrations in rats with induced diabetes. Transplant Proc. 2009; 41:1789–1793. [PubMed: 19545729]
73. Brady AC, Martino MM, Pedraza E, Sukert S, Pileggi A, Ricordi C, Hubbell JA, Stabler CL. Proangiogenic hydrogels within macroporous scaffolds enhance islet engraftment in an extrahepatic site. Tissue Eng Part A. 2013; 19:2544–2552. [PubMed: 23790218]

74. Pedraza E, Brady A-C, Fraker CA, Stabler CL. Synthesis of macro-porous poly(dimethylsiloxane) scaffolds for tissue engineering applications. J Biomater Sci Polym Ed. 2013; 24:1041–1056. [PubMed: 23683037]

75. Bernard AB, Lin C-C, Anseth KS. A microwell cell culture platform for the aggregation of pancreatic β-cells. Tissue Eng Part C Methods. 2012; 18:583–592. [PubMed: 22320435]

76. Zhao Z, Gu J, Zhao Y, Guan Y, Zhu XX, Zhang Y. Hydrogel thin film with swelling-induced wrinkling patterns for high-throughput generation of multicellular spheroids. Biomacromolecules. 2014; 15:3306–3312. [PubMed: 25072634]

77. Shinohara M, Kimura H, Montagne K, Komori K, Fujii T, Sakai Y. Combination of microwell structures and direct oxygenation enables efficient and size-regulated aggregate formation of an insulin-secreting pancreatic β-cell line. Biotechnol Prog. 30:178–187.

78. Gallego-Perez D, Higuita-Castro N, Reen RK, Palacio-Ochoa M, Sharma S, Lee LJ, Lannutti JJ, Hansford DJ, Gooch KJ. Micro/nanoscale technologies for the development of hormone-expressing islet-like cell clusters. Biomed Microdevices. 2012; 14:779–789. [PubMed: 22573223]

79. Pepper AR, Pawlick R, Gala-Lopez B, MacGillivary A, Mazzuca DM, White DJ, Toleikis PM, Shapiro AM. Diabetes Is Reversed in a Murine Model by Marginal Mass Syngeneic Islet Transplantation Using a Subcutaneous Cell Pouch Device. Transplantation. 2015; 99:2294–2300. [PubMed: 26308506]

80. Ludwig B, Rotem A, Schmid J, Weir GC, Colton CK, Brendel MD, Neufeld T, Block NL, Yavriyants K, Steffen A, Ludwig S, Chavakis T, Reichel A, Azarov D, Zimermann B, Maimon S, Balyura M, Rozenshtein T, Shabtay N, Vardi P, Bloch K, de Vos P, Schally AV, Bornstein SR, Barkai U. Improvement of islet function in a bioartificial pancreas by enhanced oxygen supply and growth hormone releasing hormone agonist. Proc Natl Acad Sci U S A. 2012; 109:5022–5027. [PubMed: 22393012]

81. Forster NA, Penington AJ, Hardikar AA, Palmer JA, Hussey A, Tai J, Morrison WA, Feeney SJ. A prevascularized tissue engineering chamber supports growth and function of islets and progenitor cells in diabetic mice. Islets. 2011; 3:271–283. [PubMed: 21847009]

82. Hussey AJ, Winardi M, Han XL, Thomas GP, Penington AJ, Morrison WA, Knight KR, Feeney SJ. Seeding of pancreatic islets into prevascularized tissue engineering chambers. Tissue Eng A. 2009; 15:3823–3833.

83. Balamurugan AN, Gu Y, Tabata Y, Miyamoto M, Cui W, Hori H, Satake A, Nagata N, Wang W, Inoue K. Bioartificial pancreas transplantation at prevascularized intermuscular space: effect of angiogenesis induction on islet survival. Pancreas. 2003; 26:279–285. [PubMed: 12657955]

84. Kriz J, Jirak D, Vilk GJ, Girman P, White DJ, Hajek M, Saudek F. Vascularization of artificial beds for pancreatic islet transplantation in a rat model. Transplant Proc. 2010; 42:2097–2101. [PubMed: 20692417]

85. Sörenby AK, Kumagai-Braesch M, Sharma A, Hultenby KR, Wernerson AM, Tibell AB. Preimplantation of an immunoprotective device can lower the curative dose of islets to that of free islet transplantation: studies in a rodent model. Transplantation. 2008; 86:364–366. [PubMed: 18645504]

86. Bowers DT, Tanes ML, Das A, Lin Y, Keane NA, Neal RA, Ogle ME, Brayman KL, Fraser CL, Botchwey EA. Spatiotemporal oxygen sensing using dual emissive boron dye-polylactide nanofibers. ACS Nano. 2014; 8:12080–12091. [PubMed: 25426706]

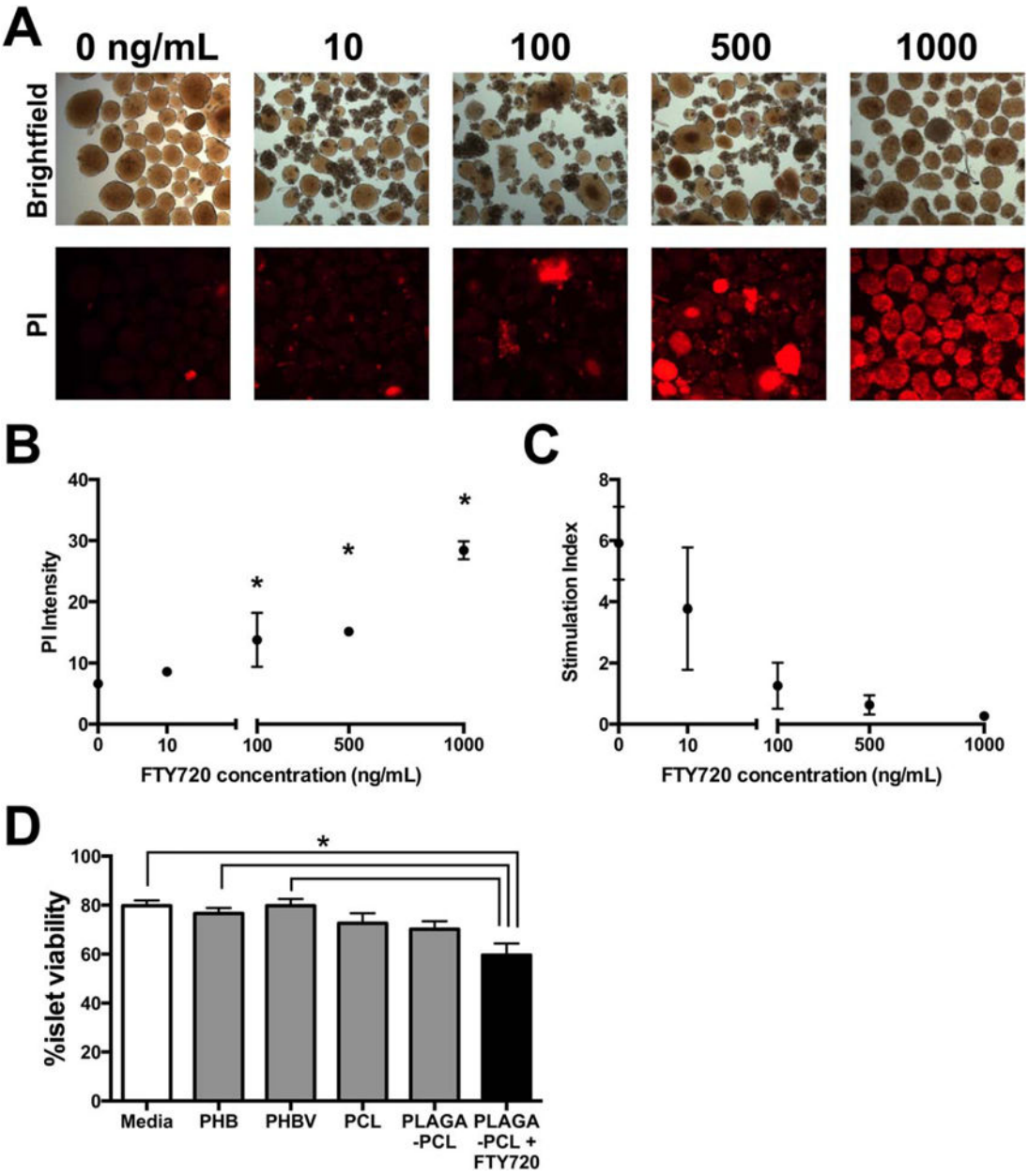

FIGURE 1.

Islet viability is reduced by high FTY720 concentration and PLGA nanofibers. (A,B) *In vitro* dose response of mouse islet apoptosis/necrosis and (C) stimulation index to increasing amounts of FTY720 added to RPMI1640 media at 37°C (n = 4,3,2,2,2 wells for 0, 10, 100, 500, 1000 ng/mL, respectively; *p < 0.05 compared to 0 ng/mL control, mean ± SEM). (D) The viability of human islets was compared when several polymers were incubated with the islets (n = 50,50,50,30,50,39 islets visually inspected for Media, PHB, PHBV, PCL, PLGA & PCL, PLGA & PCL 1:400 FTY720, respectively. *p < 0.05, mean ± SEM).

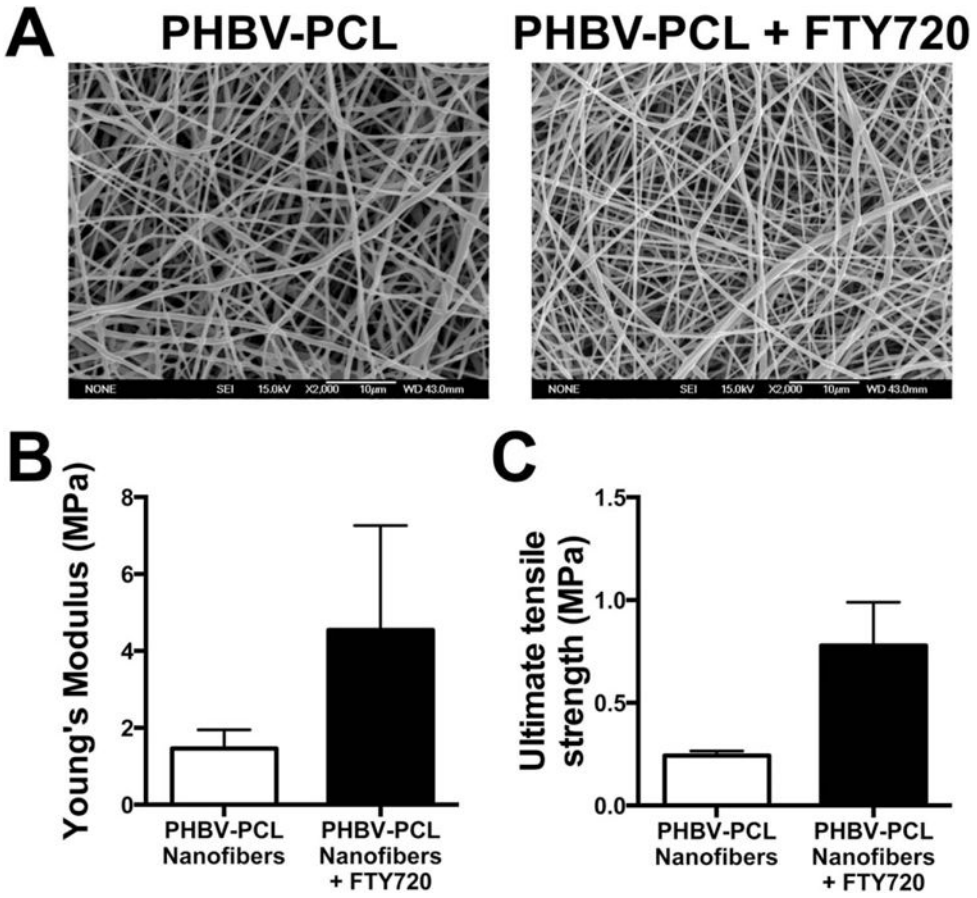

FIGURE 2.

Addition of FTY720 to PHBV-PCL nanofibers increased mechanical properties without apparent morphological changes. (A) Scanning electron micrographs of the FTY720-loaded and unloaded control electrospun nanofibers. (B) Young's modulus and (C) ultimate tensile strength of the nanofiber mats ($n = 3$ for each fiber type, mean ± SEM).

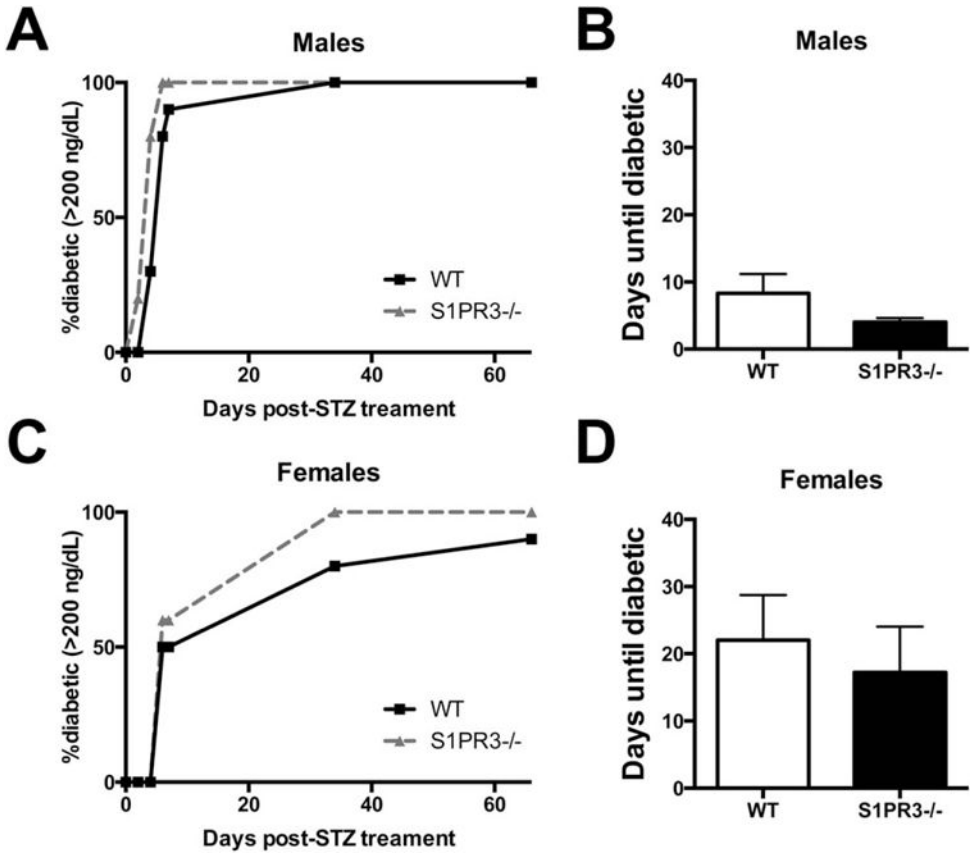

FIGURE 3.

S1P3 slows progression to streptozotocin-induced diabetes in mice. Tail vein non-fasting blood glucose values were monitored in male (A,B) and female (C,D) wild-type and S1P3−/− mice on a C57BL6 background (no significant difference, mean ± SEM). Mice were considered diabetic when glucose values were above 200 mg/dL. n = 10, 10, 5, 5 for wt male, wt female, S1P3−/− male and S1P3−/− female mice, respectively.

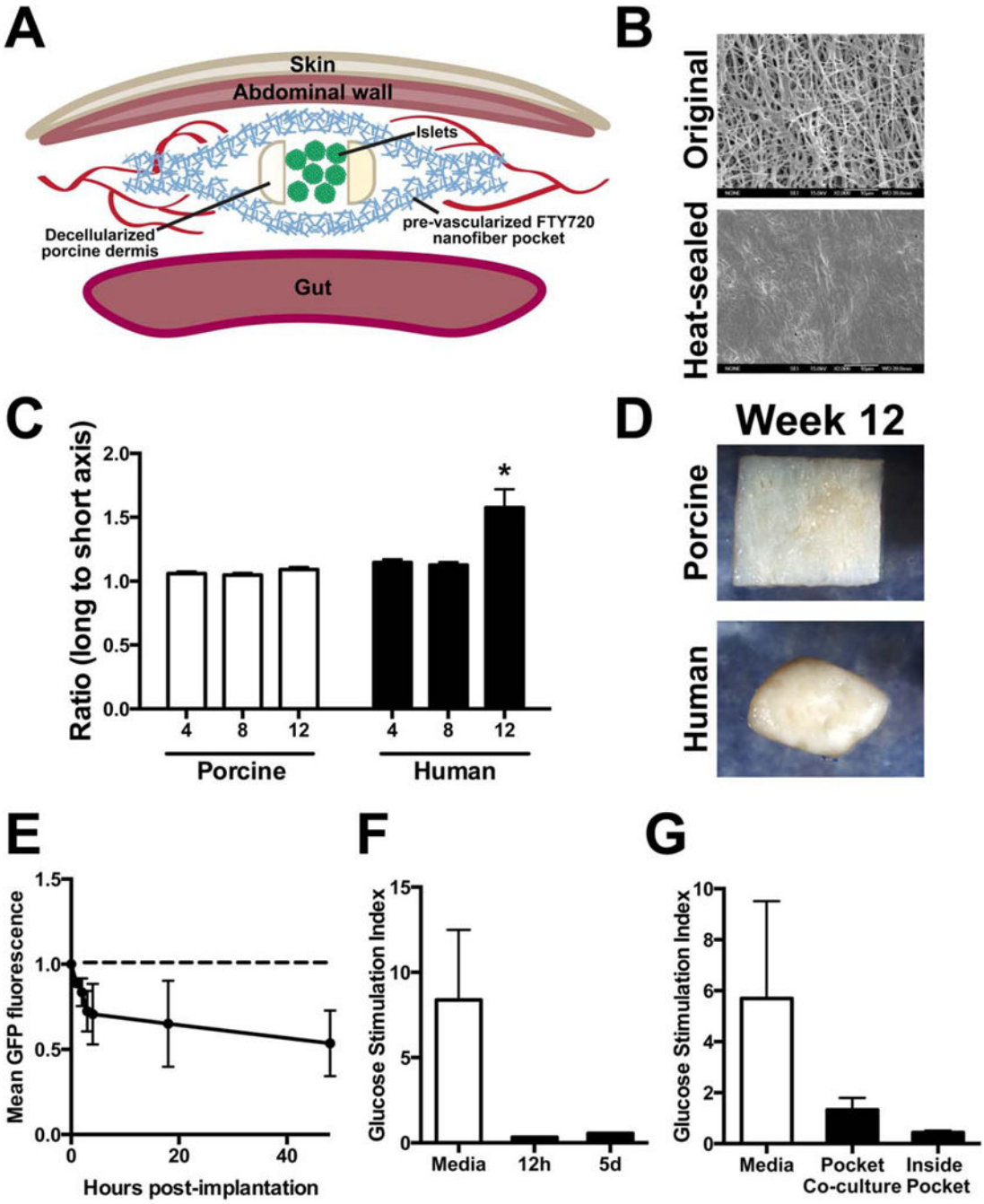

FIGURE 4.

A dimensionally stable nanofiber implant design for preconditioned pancreatic islet transplantation. (A) Diagram showing the construction of a pocket with a porcine decellularized dermis insert to maintain a separation between the nanofiber layers for the islets to occupy. (B) Scanning electron micrographs of the outside of the pocket ("unmodified") and the heat-sealed edge. (C,D) porcine decellularized dermis is dimensionally stable as seen by the ratio of the axis lengths (n = 7, 8, 10 and 8, 9, 10 for porcine and human at 4, 8, 12 weeks, respectively, *p < 0.05, mean ± SEM). (E) GFP1 murine islets have decreased fluorescence with increased time in culture inside a nanofiber

pocket. Images taken at 0, 1, 2, 3, 4, 18 and 48 h (n = 2 pockets, mean ± SEM). (F) *Ex vivo* function of mouse islets is reduced after as short as 12 h of *in vivo* implantation in a PHBV/PCL pocket in a mouse (n = 1, except n = 3 for media only that shows stimulation of islets at the 12 h timepoint after maintenance in standard suspension culture, $p > 0.05$, mean ± SEM). (G) *In vitro* experiments also showed loss of stimulated insulin secretion (n = 3 wells for each condition, salt leached PHBV-PCL + FTY720, $p > 0.05$, mean ± SEM).

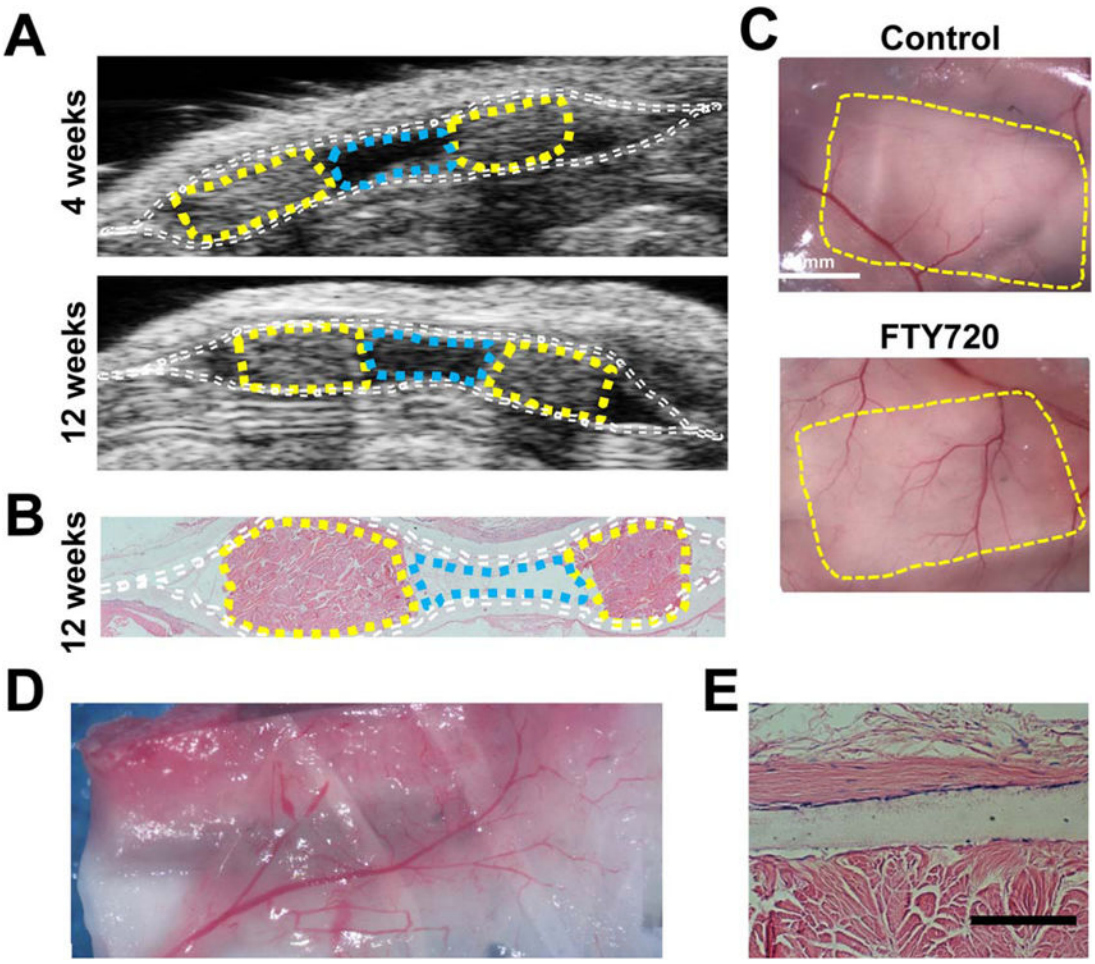

FIGURE 5.

Maintenance of implant structure imaged by ultrasound with vascularization at 12 weeks after abdominal subcutaneous implantation. (A) A subcutaneously-placed pocket monitored by ultrasound maintains a void at 4 and 12 weeks, (B) corresponding with H&E (Dotted lines: white, nanofibers; yellow, porcine decellularized dermis, cyan, void). (C) Vasculature in the intraperitoneal wall was visualized by reflection of the skin, fibers and wall upon sacrifice to compare unloaded fibers verses FTY720-loaded fibers (yellow lines: pocket edge). (D) Vascularized tissue attached to the outside of the FTY720-loaded nanofiber pocket after implantation and integration in the peritoneal cavity. (E) Histological (H&E) section of an FTY720-loaded membrane next to the structural support showing a lack of vessel penetration, scale bar 100 μm.

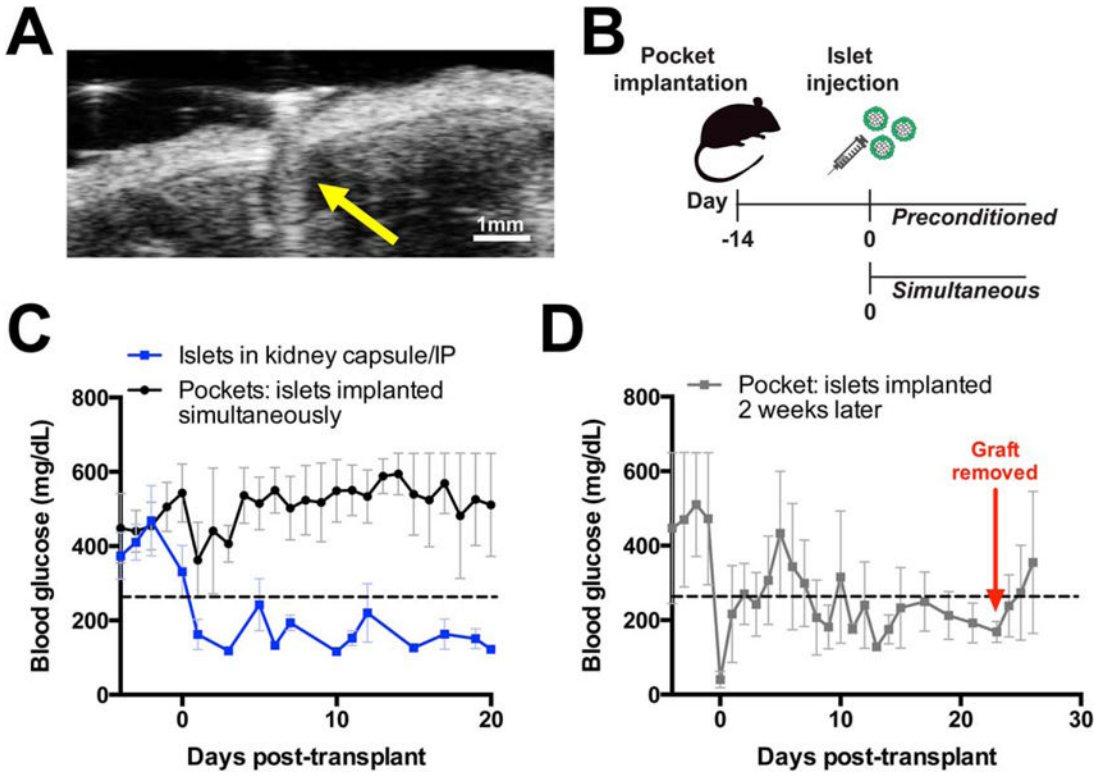

FIGURE 6.

Islets transplanted into a 14 day preconditioned nanofiber pocket restore normoglycemia in preliminary transplants. (A) Minimally invasive injection of islets into the pocket can be ultrasound-assisted (yellow arrow: 28G needle). (B) Preconditioning scheme introduces islets 2 weeks after the nanofiber encapsulation device. (C) Syngeneic islets transplanted without nanofibers were placed under the kidney capsule or freely floating in the intraperitoneal cavity resulting in blood glucose reduction (blue line, $n = 5$, mean ± SEM). Islets were transplanted inside a FTY720 PHBV/PCL salt-leached nanofiber pocket at the time of implantation without correction of blood glucose (black line, $n = 5$, mean ± SEM). (D) Islets introduced to a FTY720 PHBV/PCL salt-leached nanofiber preconditioned pocket reach normoglycemia ($n = 2$, mean ± SEM). Glucose increase beyond day 24 is attributed to the islet containing implant being removed, indicating glucose control was derived from transplanted cells.

TABLE I

Parameters for Production of Electrospun Polymer Nanofibers

Polymer	FTY720 (w/w)	Solvent	Concentration (w/v)	Working Distance (cm)	Voltage (kV)	Flow Rate (mL/hr)
PHB		HFP	1.4	15	7	1.5
PHBV		HFP	6.5	15–20	10	1
PCL		THF:DMF	14	20	14	1
PLGA-PCL (1:1 w/w)		3:1 (v/v) chloroform: methanol	18	10	19	1
PLGA-PCL + FTY	1:200	3:1 (v/v) chloroform: methanol	20	15	19	1
PHBV-PCL (1:1 w/w)		3:1 (v/v) chloroform: methanol	18	14	19	1
PHBV-PCL + FTY	1:200	3:1 (v/v) chloroform: methanol	18	14	19	1

J Biomed Mater Res B Appl Biomater. Author manuscript; available in PMC 2018 February 01.

TABLE II

Contact Angle of Two Liquids on FTY720 Loaded and Unloaded PHBV-PCL Fibers (n = 3 Per Sample)

	Liquid	Angle (Degrees)
PHBV-PCL	Water	116.1 ± 86.6
	Glycerin	121.3 ± 85.4
PHBV-PCL FTY720	Water	49.5 ± 86
	Glycerin	74.3 ± 87.1